

**AD-A240 764**



**RADC-TR-90-186**  
**In-House Report**  
July 1990



# **A THINNED HIGH FREQUENCY LINEAR ANTENNA ARRAY TO STUDY IONOSPHERIC STRUCTURE**

**Anthony J. Gould, Capt, USAF**



*APPROVED FOR PUBLIC RELEASE; DISTRIBUTION UNLIMITED.*

**91-10962**

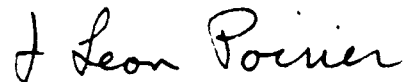


**Rome Air Development Center**  
**Air Force Systems Command**  
**Griffiss Air Force Base, NY 13441-5700**

This report has been reviewed by the RADC Public Affairs Division (PA) and is releasable to the National Technical Information Services (NTIS). At NTIS it will be releasable to the general public, including foreign nations.

RADC-TR-90-186 has been reviewed and is approved for publication.

APPROVED:



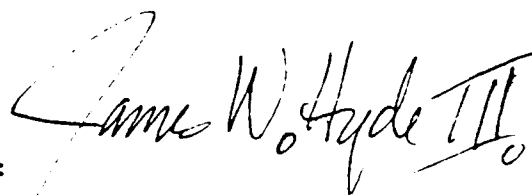
J. LEON POIRIER, Chief  
Applied Electromagnetics Division  
Directorate of Electromagnetics

APPROVED:



JOHN K. SCHINDLER  
Director of Electromagnetics

FOR THE COMMANDER:



JAMES W. HYDE III  
Directorate of Plans & Programs

If your address has changed or if you wish to be removed from the RADC mailing list, or if the addressee is no longer employed by your organization, please notify RADC (EECP) Hanscom AFB MA 01731-5000. This will assist us in maintaining a current mailing list.

Do not return copies of this report unless contractual obligations or notices on a specific document require that it be returned.

RADC-TR-90-186  
In-House Report  
July 1990

A THINNED HIGH FREQUENCY LINEAR ANTENNA ARRAY TO  
STUDY IONOSPHERIC STRUCTURE

ANTHONY J. GOULD, CAPT, USAF

ERRATA

TITLE ON PAGE 31 SHOULD READ REFERENCES -- WORD IS SPELLED INCORRECTLY.

## REPORT DOCUMENTATION PAGE

Form Approved  
OMB No. 0704-0188

1a. REPORT SECURITY CLASSIFICATION UNCLASSIFIED		1d. RESTRICTIVE MARKINGS N/A	
2a. SECURITY CLASSIFICATION AUTHORITY N/A		3. DISTRIBUTION / AVAILABILITY OF REPORT Approved for public release; distribution unlimited.	
2b. DECLASSIFICATION / DOWNGRADING SCHEDULE N/A			
4. PERFORMING ORGANIZATION REPORT NUMBER(S) RADC-TR-90-186		5. MONITORING ORGANIZATION REPORT NUMBER(S)	
6a. NAME OF PERFORMING ORGANIZATION Rome Air Development Center	6b. OFFICE SYMBOL (If applicable) EECP	7a. NAME OF MONITORING ORGANIZATION	
6c. ADDRESS (City, State, and ZIP Code) Hanscom AFB, MA 01731-5000		7b. ADDRESS (City, State, and ZIP Code)	
8a. NAME OF FUNDING / SPONSORING ORGANIZATION	8b. OFFICE SYMBOL (If applicable)	9. PROCUREMENT INSTRUMENT IDENTIFICATION NUMBER N/A	
8c. ADDRESS (City, State, and ZIP Code)		10. SOURCE OF FUNDING NUMBERS	
		PROGRAM ELEMENT NO. 62702F	PROJECT NO. 4600
		TASK NO. 16	WORK UNIT ACCESSION NO. 10
11. TITLE (Include Security Classification) A Thinned High Frequency Linear Antenna Array to Study Ionospheric Structure			
12. PERSONAL AUTHOR(S) Gould, Anthony J., Capt. USAF			
13a. TYPE OF REPORT In-House	13b. TIME COVERED FROM 3/89 TO 3/90	14. DATE OF REPORT (Year, Month, Day) 1990 July	15. PAGE COUNT 38
16. SUPPLEMENTARY NOTATION			
17. COSATI CODES		18. SUBJECT TERMS (Continue on reverse if necessary and identify by block number)	
FIELD	GROUP	Antenna Array	
20	14	HF	
17	09	Ionospheric Propagation	
19. ABSTRACT (Continue on reverse if necessary and identify by block number) The design, modeling, and performance measurements of a high frequency (HF) linear antenna array with 36 sensors is reported. The array was designed to achieve a narrow azimuthal beamwidth while maintaining grating lobes 10 dB below the main beam during a $\pm 30^\circ$ scan in azimuth. The configuration chosen utilizes two active vertical monopole elements and two parasitic backpoles to form a subarray. The subarrays, or sensors, are spaced at distances greater than half a wavelength to provide a large effective array aperture while the elemental radiation pattern, provided by the subarrays, suppresses the grating lobe as the array is scanned. Radiation patterns for the array were determined using three independent techniques: theoretical calculation, computer modeling using the Numerical Electromagnetics Code (NEC), and measurement of the fielded antenna. Results showed close agreement in antenna performance among the three methods of pattern determination. The three step process of theory, numerical modeling and measurement appears to be an optimum approach to antenna design.			
20. DISTRIBUTION/AVAILABILITY OF ABSTRACT <input checked="" type="checkbox"/> UNCLASSIFIED/UNLIMITED <input type="checkbox"/> SAME AS RPT. <input type="checkbox"/> DTIC USERS		21. ABSTRACT SECURITY CLASSIFICATION Unclassified	
22a. NAME OF RESPONSIBLE INDIVIDUAL Anthony J. Gould, Capt, USAF		22b. TELEPHONE (Include Area Code) (617) 377-4904	22c. OFFICE SYMBOL RADC/EECP

Accession For	
NTIS CR&I	✓
DTIC TAB	□
Unannounced	□
Justification	
By	
Distribution/	
Availability Codes	
Dist	Availability Codes
A-1	

## Contents

1. RADC HIGH FREQUENCY TEST FACILITY	1
2. LINEAR ANTENNA ARRAY	2
2.1 Design Objectives	2
2.2 Verona Array Description	2
3. THEORETICAL METHODS AND CONSIDERATIONS	3
3.1 Calculation of Theoretical Radiation Patterns	3
3.2 Simple Vertical Monopole Element	3
3.3 Two-Element Subarrays	7
3.3.1 Two-Active Elements Phased Broadside	7
3.3.2 Active Element and Backpole Phased Endfire	7
3.4 Design of Subarray Dimensions	10
3.5 Calculation of the Array Factor	12
3.6 Pattern Multiplication of Array Factor and Subarray Pattern	12
3.7 Grating Lobe Reductions	12
4. CALCULATIONS USING NUMERICAL ELECTROMAGNETICS CODE (NEC)	16
4.1 Introduction to NEC	16
4.2 Far-Field Patterns Calculated with NEC	16
4.2.1 Vertical Monopole Over Perfect Ground	16
4.2.2 Two Active Elements	16
4.2.3 Monopole with Backpole	16
4.2.4 Full Subarray	20
4.2.5 Model of the Full Array	20
5. FIELD MEASUREMENTS	20
5.1 Introduction and Techniques	20
5.2 Measurement of the Subarray Pattern	24
5.3 Measurement of the Array Pattern	24



## Contents

6. ARRAY DESCRIPTION	24
7. DISCUSSION	29
REFERENCES	31

## Illustrations

1. Verona Linear Array Coverage	3
2. Subarray Configuration for the Verona Linear Array	4
3. Verona Linear Antenna Array Setup	6
4. Theoretical Elevation Patterns for a Vertical Monopole	8
5. Theoretical Azimuthal Far-Field Pattern for Two Vertical Monopole Phased Broadside	9
6. Theoretical Pattern for One Active Element and One Backpole Phased Endfire	11
7. Theoretical Azimuthal Far-Field Pattern for a Subarray with Two Active Elements and Two Backpoles	13
8. Array Factor, Subarray Pattern, and Resultant Radiation Pattern from Pattern Multiplication of Array Factor with the Subarray Pattern	14
9. Array Factor, Subarray Pattern, and Resultant Radiation Pattern for Linear Array Scanned 20 Degrees Off Broadside	15
10. Elevation Radiation Pattern for a Simple Vertical Monopole Over Perfect and Finite Ground Planes Calculated with the NEC Modeling Program	17
11. Azimuthal Pattern for a Two Element Subarray Phased Broadside Calculated with NEC	18
12. Azimuthal Radiation Pattern for a Two Element Subarray Phased Endfire Calculated Using the NEC Routine	19
13. NEC Azimuthal Radiation Pattern for a Four Element Subarray Including Two Active Elements and Two Backpoles	21
14. NEC Radiation Pattern for a Linear Array of 15 Subarrays, Including Two Active Elements and Two Backpoles. Zero degree scan angle	22
15. NEC Radiation Pattern for a Linear Array of 15 Subarrays, with a 32 dB Cosine Squared Weighting Taper	23

## Illustrations

16. Measured Azimuthal Radiation Pattern for the Fielded Four Element Subarray	25
17. Measured 56 Element Linear Array Radiation Pattern Using the Ava Tx. Site as a source with a 32 dB cosine square weighting	26
18. Schematic of One Active Element	27
19. Subarray Schematic	28

## Table

1. Parameter Values from Each of Three Techniques	29
---	----

## **A Thinned High Frequency Linear Antenna Array to Study Ionospheric Structure**

### **1. RADC HIGH FREQUENCY TEST FACILITY**

RADC/EECP has assembled a high frequency (HF) radar and communication test facility at the RADC Verona Test Annex, Verona, NY. The system consists of a set of 36 digital HF radio receivers controlled by a DEC Micro-Vax II computer and an extended aperture linear antenna array. The mission of the facility is two-fold: first, investigate propagation mechanisms and limits imposed on HF systems by the ionosphere; second, explore digital processing techniques such as adaptive sidelobe cancellation, narrowband noise excision, and time domain noise excision that could lead to improvement of current and future Air Force surveillance and communications systems which use the HF frequency band.

The radar system at Verona converts the HF signals from the 36 antenna sensors of the linear array to a digital format using A/D converters in each of 36 receivers. Antenna calibration, beamforming, and all radar processing is carried out by the system computer during post processing. This report details only the linear antenna array. Information concerning the receivers, operational methods, and data processing will be presented in a separate report.

The purpose of equipping the test facility with an extended aperture linear array was to create a high resolution probe to study ionospheric structure and use this knowledge to improve backscatter radar techniques.

---

(Received for Publication 1 July 1990)

## **2. LINEAR ANTENNA ARRAY**

### **2.1 Design Objectives**

The HF test facility at Verona was designed to measure ionospheric backscatter signals with high resolution and record the receiver baseband digitally. There are many sources of ionospheric clutter; radio aurora, F-region irregularities, equatorial irregularities, and others. All these mechanisms contribute interference that is known to degrade HF propagation performance. Measurements using the linear antenna array will help provide the data needed to evaluate the effectiveness of digital processing techniques to reduce interference caused by the irregularities at the high latitudes. The backscatter data will also be used to characterize or map ionospheric phenomena in the high latitudes. This mapping will help determine the spatial and temporal extent of ionospheric irregularities.

The frequency range of the receiver system is 5-30 MHz which encompasses most of the HF band. However, high intensity phenomena are usually present during nighttime operation when the ionosphere dictates that the most effective operating frequencies are at the low end of the HF band. Therefore, 6-12 MHz was used as the design operating band for the linear array. While the array will certainly work to some extent over a much larger frequency band, the array was tuned to perform best in the 6-12 MHz region. With this criterion in mind, the 36 element linear array was configured to obtain maximum resolution in azimuth while still maintaining low sidelobe control over the operating frequency band of 6-12 MHz.

A random array of elements spaced over a large aperture is one way to approach this problem. However, it was decided not to use this method for several reasons. First, increased signal processing is necessary to reduce the sidelobes to levels comparable to a periodic array. Secondly, the mainbeam pattern and sidelobe levels are difficult to predict during all operating situations. Finally, the array was to retain as much commonality as possible with other existing HF antenna systems.

A linear array of widely spaced (greater than half wavelength) directional elements was chosen as a practical solution to the problem. Such an array provides a wide aperture that results in a narrow beamwidth in azimuth and also provides good sidelobe control. A wider aperture is possible using subarrays of monopole elements that control grating lobes as the array is scanned. Backpoles placed a quarter wavelength behind each active element provide increased directivity of the array in the forward direction. While a backscreen is more effective, environmental concerns and colocation with other experiments on the selected site currently prohibit use of a large backscreen. The geographic coverage area of the array is shown in Figure 1. Note that the coverage area includes a large overlap of the area associated with the nighttime auroral oval.

### **2.2 Verona Array Description**

The linear HF antenna array at Verona NY is composed of 36 subarrays with a spacing of 20 m between centers of each subarray. This elemental spacing corresponds to 0.8 wavelength at the upper design frequency of 12 MHz. The dimensions and components of the subarrays are shown in Figure 2. The main idea in the subarray design process was to use a given number of monopoles as the basic components to create a directional element. Two monopole elements, placed a half wavelength apart ( $D_2 = 12.5$  m), in a broadside configuration provided forward directivity and reduced the energy

# VERONA LINEAR ARRAY COVERAGE

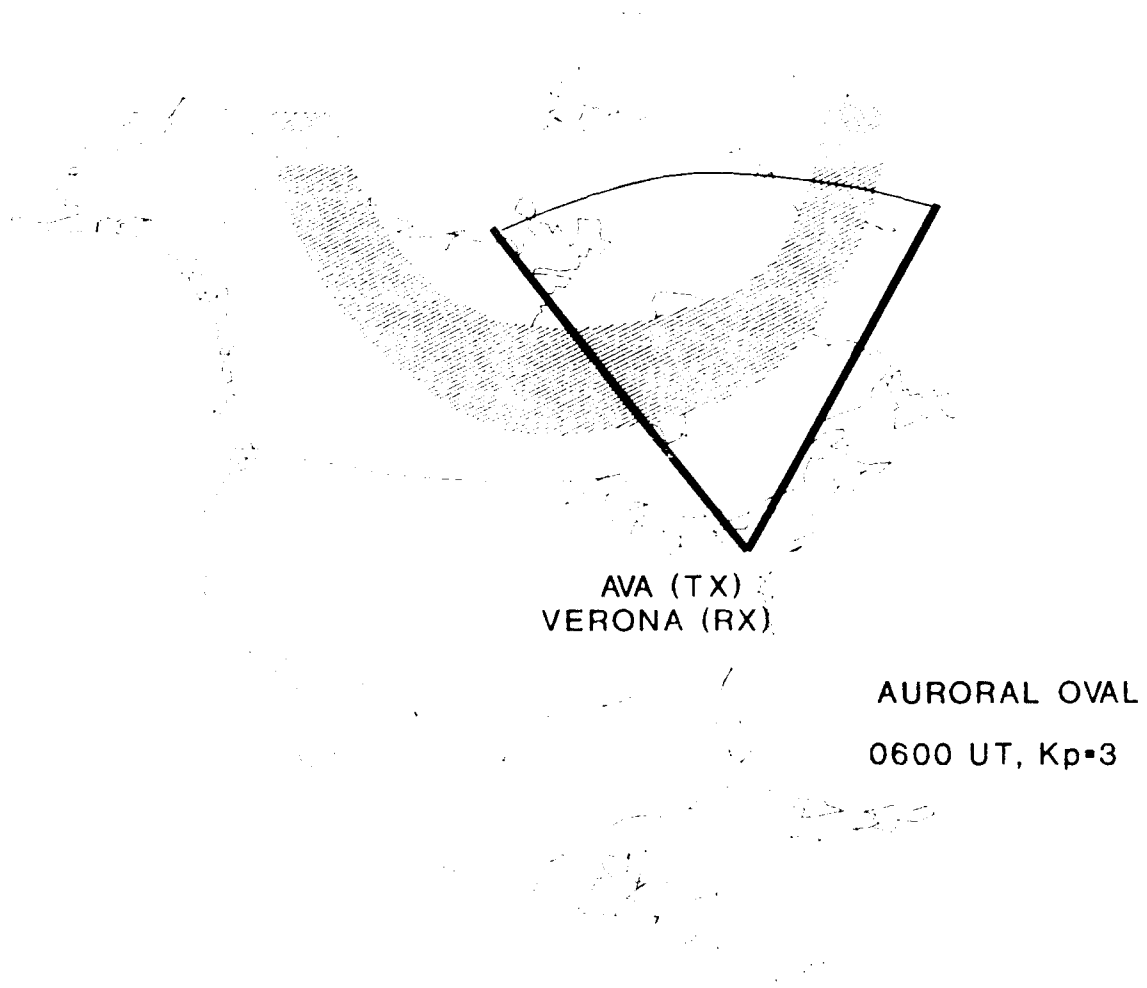


Figure 1. Verona Linear Array Coverage

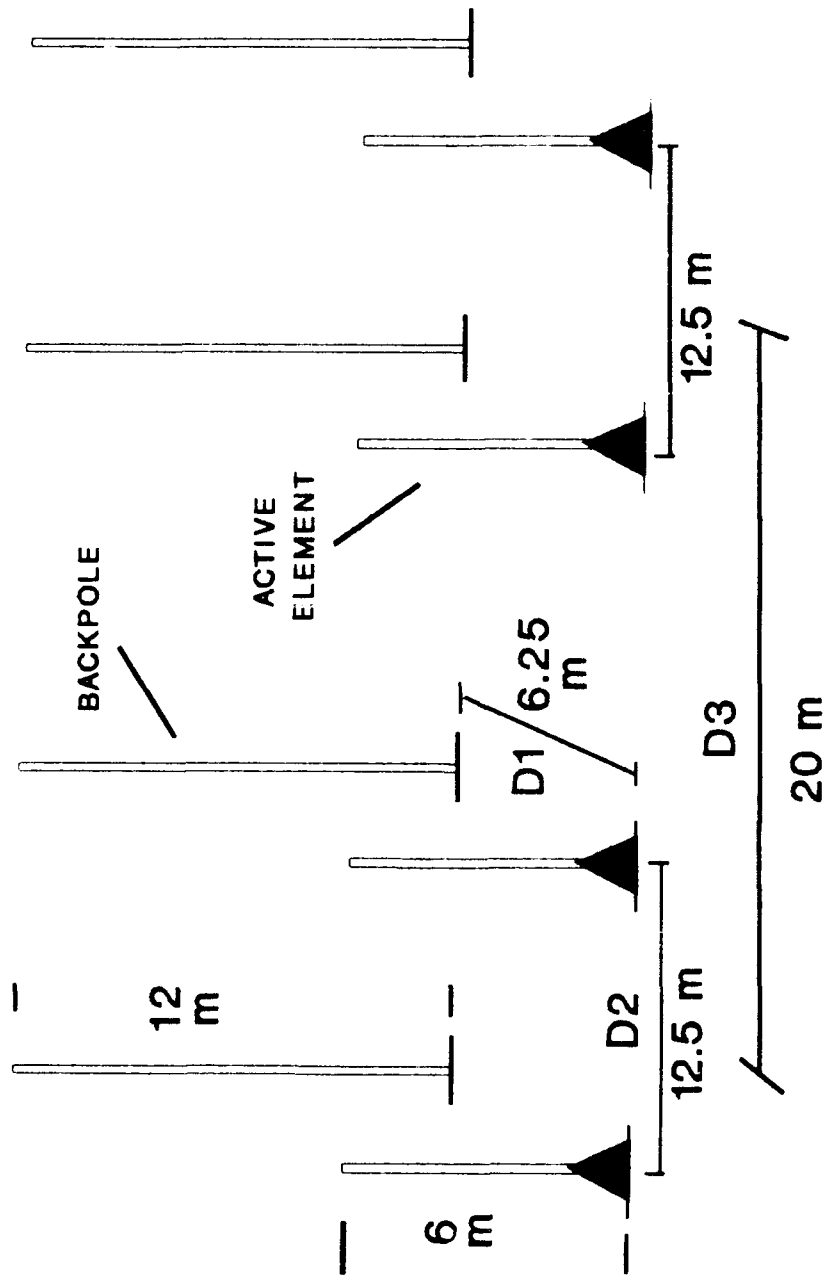


Figure 2. Subarray Configuration for the Verona Linear Array

received from signals arriving from the direction parallel to the array. The 6 m height of these two elements was chosen to keep the element length near a quarter wavelength of the operating frequencies. A 12 m backpole was placed a quarter wavelength ( $D_1 = 6.25$  m) behind each of the 6 m elements. A height of 12 m was chosen to keep the backpoles greater than a quarter wavelength even at the low end of the operating band. The four monopoles acting together as a subarray provide forward directivity and wide nulls at angles of  $\pm 90$  degrees and 180 degrees. The spacing between the subarrays ( $D_3$ ) was determined from the constraint of reducing the grating lobe by 10 dB when the array is scanned 30 degrees at a frequency of 12 MHz.

A schematic of the linear array setup is shown in Figure 3. Several parameters are included in this figure to point out the major features of the array including its length, spatial orientation, operating frequency band, scan limits, and minimum beamwidth.

### 3. THEORETICAL METHODS AND CONSIDERATIONS

#### 3.1 Calculation of Theoretical Radiation Patterns

Far-field azimuthal radiation patterns were calculated at several stages of the antenna array development. These stages included a simple monopole element, two elements phased broadside, two elements phased broadside, two elements phased endfire, a four element subarray, and the 36 element linear array.

The effect of the ground upon the vertical field patterns was carefully considered. While a finite ground might have little effect on the input impedance of a vertical monopole, the field pattern can be greatly influenced by the ground conductivity. Fortunately for the antenna, (and unfortunately for the experimenters), the land at Verona is a swamp. Ground conductivity for this area is very high. A conductivity value of  $\sigma = 0.1$  mhos/m and a relative dielectric constant of  $\epsilon = 30$  were used for all calculations. These values were chosen from literature as being consistent for a marshy ground.<sup>1</sup> While this is by no means a perfectly reflective ground it improves the antenna performance at receive angles close to the horizon. In addition, a ground screen was installed in front of the array to ensure a stable impedance for the antenna. The ground screen consisted of two 22 gauge aluminum clad wires extending 75 m in front of each element. Field calculations were made with the assumption of an infinite and perfect ground plane.

#### 3.2 Simple Vertical Monopole Element

The first antenna structure investigated was a vertical monopole over a perfect ground plane. This antenna has a radiation pattern similar to a vertical dipole in free space and is therefore omnidirectional in the azimuthal plane. The elevation field pattern for a vertical monopole has been extensively calculated in the past and verified for nearly all situations.<sup>2</sup> Parameters that influence the pattern are ground conductivity, element length, element radius, and operating frequency.

- 
1. Jordan, E., Ed. (1986) *Reference Data for Radio Engineers*, Howard W. Sams & Co.
  2. Kraus, J.D. (1984) *Electromagnetics*, 3rd Ed., McGraw-Hill, p. 518.

FREQ. 6-12 MHZ  
10° E OF N TRUE

2.5° BEAMWIDTH\*  
+/- 30° SCAN

\* AT 12 MHZ

72 MONOPOLES

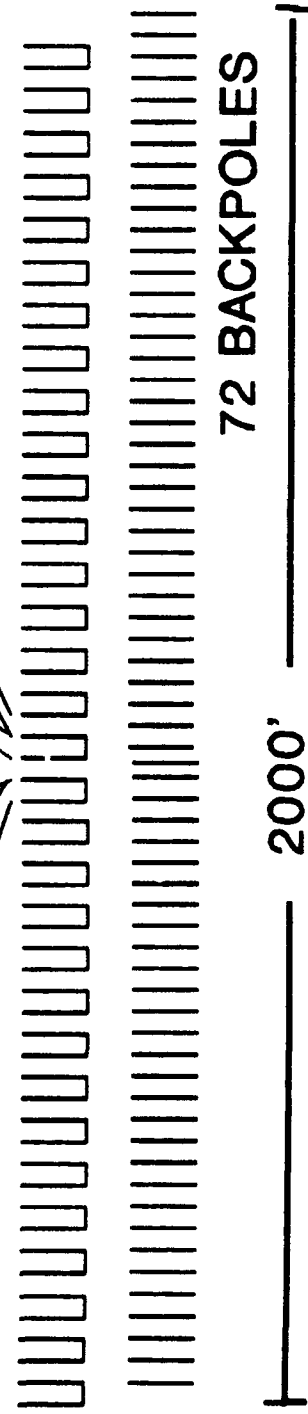


Figure 3 VLF Linear Antenna Array Setup

Elevation patterns are shown in Figure 4 for a thin, 6 m monopole over a perfect ground plane and also with  $\sigma = 0.1$  and  $\epsilon = 30$ . Note that the loss in gain for the antenna over a finite conducting ground becomes critical only at angles close to the horizon, (greater than 85 degrees). This strongly suggests good low angle performance for the Verona linear antenna, which allows for long range OTH radar operation.

### 3.3 Two-Element Subarrays

#### 3.3.1 TWO-ACTIVE ELEMENTS PHASED BROADSIDE

The next step in the pattern shaping processing was to add a second monopole and phase the resultant pair to increase the gain at broadside (0 degrees) while placing a null in the endfire (90 degrees, 270 degrees) direction. The azimuth pattern for a two-element broadside array of point sources with  $D_2 = 0.5\lambda$  is described by Eq. (1).

$$E(\phi) = 2 \cdot \sin \frac{(k \cdot D_2 \cdot \cos(\phi))}{2} \quad (1)$$

where

$$k = \frac{2\pi}{\lambda}$$

The pattern resulting from Eq. (1) is shown in Figure 5. Note the nulls in the  $\pm 90$  degrees directions and maximum directivity to the front and rear of the array.

#### 3.3.2 ACTIVE ELEMENT AND BACKPOLE PHASED ENDFIRE

The next step in the pattern shaping process was the addition of parasitic backpoles placed a quarter wavelength ( $D_1 = 6.25$  m) behind each active element. One active element and one parasitic backpole were considered as an endfire array. A backscreen greater than a quarter wavelength in height (at 6 MHz) and placed one quarter wavelength behind the active radiators acts as a reflector. This reflector increases gain in the forward direction by several decibels and provides nulling of any signals arriving from behind the array. Such a backscreen would be over 12 m high and 700 m long. Environmental constraints and other on-going experiments conducted at the Verona test site prevented building such a structure. However, the antenna gained significant benefit from a passive or parasitic element placed one quarter wavelength behind each active element. These "backpole" elements are connected only to the ground screen and to a copper grounding stake driven 1.2 m deep into the earth beside each backpole. The increase in electric field intensity as a function of azimuth angle  $\phi$ , of one active monopole with a parasitic backpole, is derived by Kraus<sup>3</sup> and shown by Eq. (2).

---

3. Kraus, J.D. (1988) *Antennas*, McGraw-Hill.

VERTICAL MONOPOLES: 6 m HEIGHT, 12 MHz, 1. PERFECT GRND. 2.  $E = 0.1$ ,  $D = 30$ .

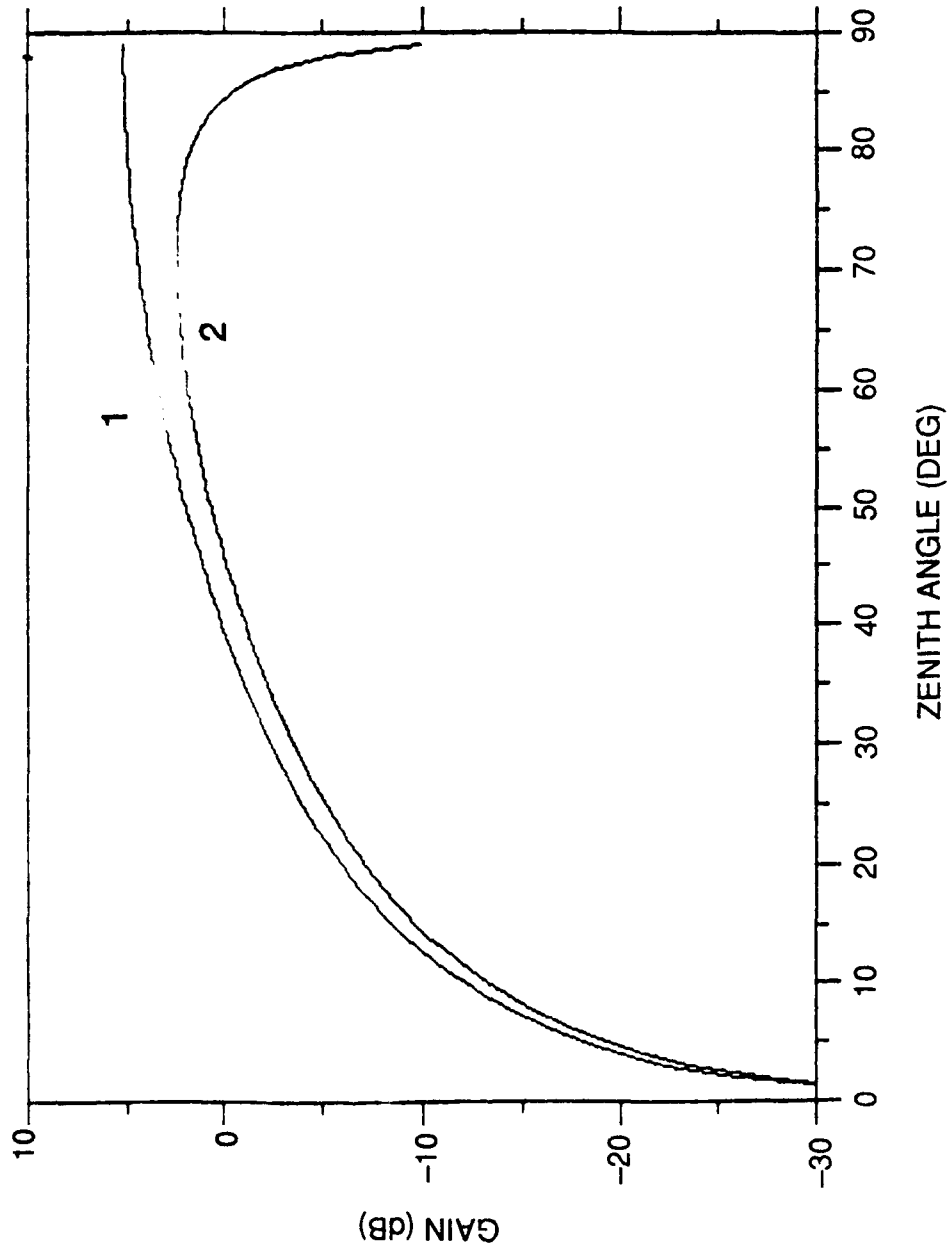


Figure 4. Theoretical Elevation Patterns for a Vertical Monopole

THEORETICAL PATTERN FOR TWO VERTICAL MONOPOLES PHASED BROADSIDE

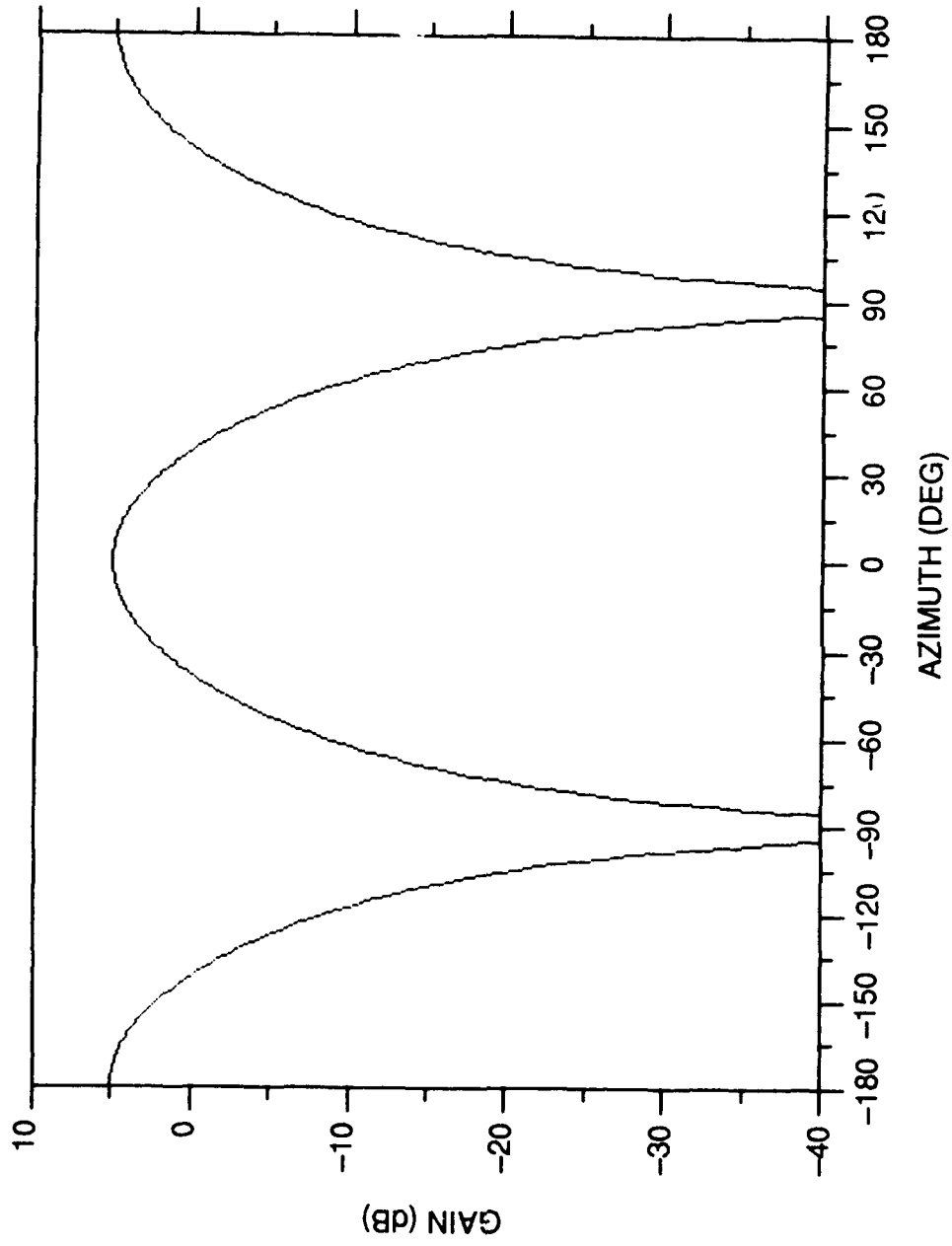


Figure 5. Theoretical Azimuthal Far-Field Pattern for Two Vertical Monopole Phased Broadside

$$G(\phi) = \sqrt{\frac{R_{11} + R_{1L}}{R_{11} + R_{1L} - |Z_{12}^2/Z_{22}| \cos(2 \cdot \tau_m - \tau_2)}} \quad (2)$$

$$\times \left[ 1 + \left| \frac{Z_{12}}{Z_{22}} \right| \cdot \varepsilon + d_r \cdot \cos(\phi) \right]$$

where

$R_{11}$  = Self resistance of a vertical antenna element

$R_{1L}$  = Effective loss resistance of a single element

$R_{12} + jX_{12} = Z_{12}$  = Mutual impedance, elements 1 and 2

$R_{22} + jX_{22} = Z_{22}$  = Backpoles self-impedance

$$\tau_m = \arctan \frac{X_{12}}{R_{12}}, \quad \tau_2 = \arctan \frac{X_{22}}{R_{22}}$$

$d_r$  = Spacing between elements

Note in Eq. (2), that as the impedance of the backpole element ( $Z_{22}$ ) is increased the effect of the backpole decreases and the gain approaches that of a single active element ( $G(\phi)=1$ ). The effectiveness of the backpole therefore depends to a large extent upon its length. Also, it can be shown from Eq. (2) that when the backpole is made longer than  $\lambda/4$  it acts as a reflector, and when it is shorter than  $\lambda/4$  it becomes capacitive and behaves as a director. Changing frequency will alter the performance of the array since this corresponds to changing the dimensions of the array in terms of wavelength.

Complete cancellation of the signal arriving from 180 degrees is possible only if dimensions and physical orientation of the array are perfect. Signals arriving from angles not exactly 180 degrees are never completely cancelled. This arrangement does however, predict a significant increase in the forward (0 degrees) directivity and a decrease in directivity to the rear (180 degrees). The field pattern for one active element and one backpole in a two-element endfire configuration array of point sources with ( $D_1 = \lambda/4$ ) is described by Eq. (3) and illustrated in Figure 6. The pattern shows the largest gain in the forward direction and indicates a null in the 180 degree direction.

$$E_1(\phi) = 2 \cdot E_o \cdot \cos \frac{(k \cdot D_1 \cdot \sin(\phi))}{2} \quad (3)$$

where

$D_1$  = Distance in wavelength between elements

$\phi$  = Azimuthal scan angle from broadside

$$k = \frac{2\pi}{\lambda}$$

### 3.4 Design of Subarray Dimensions

The last step in elemental beam shaping is to combine the broadside and endfire configurations to create the final subarray. Combination of the broadside and endfire patterns through pattern

THEORETICAL PATTERN FOR ONE ACTIVE ELEMENT AND ONE BACKPOLE PHASED ENDFIRE

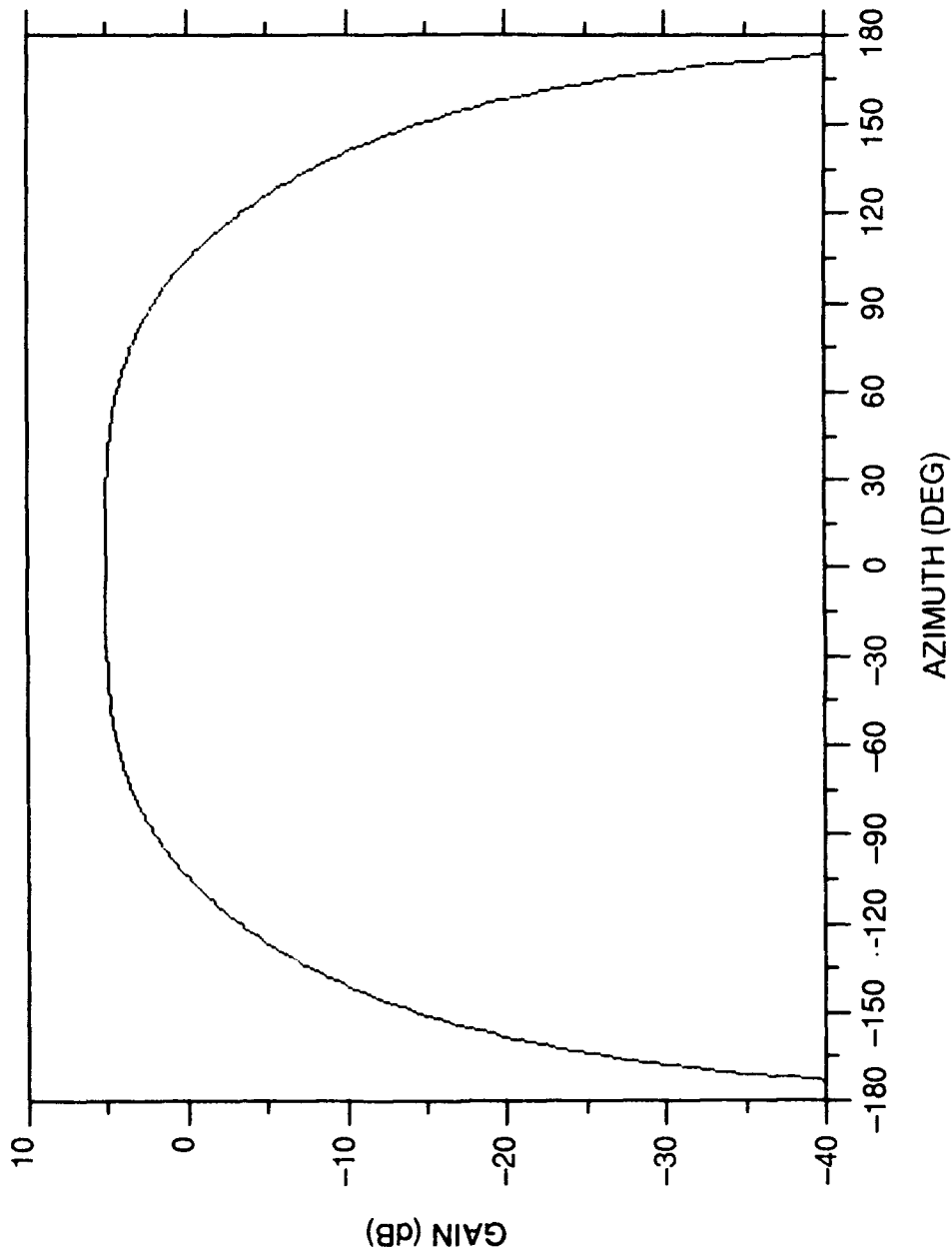


Figure 6. Theoretical Pattern for One Active Element and One Backpole Phased Endfire

multiplication results in the subarray pattern formed by the two active elements and the two passive backpoles. The pattern for this setup is shown in Figure 7. The main element gain is shown to be in the forward direction. Nulls are located in the  $\pm 90$  degree and 180 degree directions. This pattern is considered to be the theoretical element pattern.

### 3.5 Calculation of the Array Factor

The far-field array factor for a linear array of 36 isotropic point sources is described by Eq. (4). The field pattern for the array factor with  $N = 36$ ,  $D_3 = 0.8\lambda$ , and  $\phi_0 = 0$  is shown by the plot in Figure 8. This pattern is for a uniform array where all 36 elements are weighted equally. The peak of the first sidelobe is 13.2 dB below the main beam. The 3 dB beamwidth is approximately 2.5 degrees.

$$E_{\text{array}} = \frac{\sin [\pi \cdot N \cdot D_3 (\sin (\phi) - \sin (\phi_0))]}{N \cdot \sin [\pi \cdot D_3 (\sin (\phi) - \sin (\phi_0))]} \quad (4)$$

where

$N$  = Total number of elements

$D_3$  = Distance between array sensors in wavelengths

### 3.6 Pattern Multiplication of Array Factor and Subarray Pattern

A broadside (0 degree scan) far-field array pattern for the thinned linear antenna array is also shown in Figure 8. It was calculated by multiplying the subarray (element) pattern (also shown in Figure 8) by the array factor. Uniform amplitude weighting was used in calculating this pattern. Characteristic 13 dB sidelobes are seen on either side of the main beam. However, now a broad subarray pattern has been placed over the array factor. This results in higher directivity in the forward direction and nulls at angles of  $\pm 90$  degrees, and 180 degrees.

### 3.7 Grating Lobe Reductions

A plot of the array factor when the array is scanned off broadside by 20 degrees is shown in Figure 9. Note the grating lobes that have moved into the pattern. They are located at -120 degrees, -80 degrees and 160 degrees and are equal in amplitude to the main beam of the pattern now at 20 degrees. Another plot in Figure 9 shows the total array pattern. Notice that the amplitude of the grating lobes relating to the main beam has been lowered significantly by the element pattern with the nearest one at -80 degrees now lower by 16 dB. This reduction in grating lobes of the array by using directive subarrays has permitted the aperture of the array to be increased from 437.5 m for the usual  $\lambda/2$  spacing between elements to 700 m for 0.8 wavelengths between elements. This corresponds to a decrease in beamwidth from 4 degrees to 2.5 degrees at the 12 MHz design frequency.

FIELD PATTERN FOR FULL SUBARRAY OF TWO ACTIVE ELEMENTS AND TWO BACKPOLES

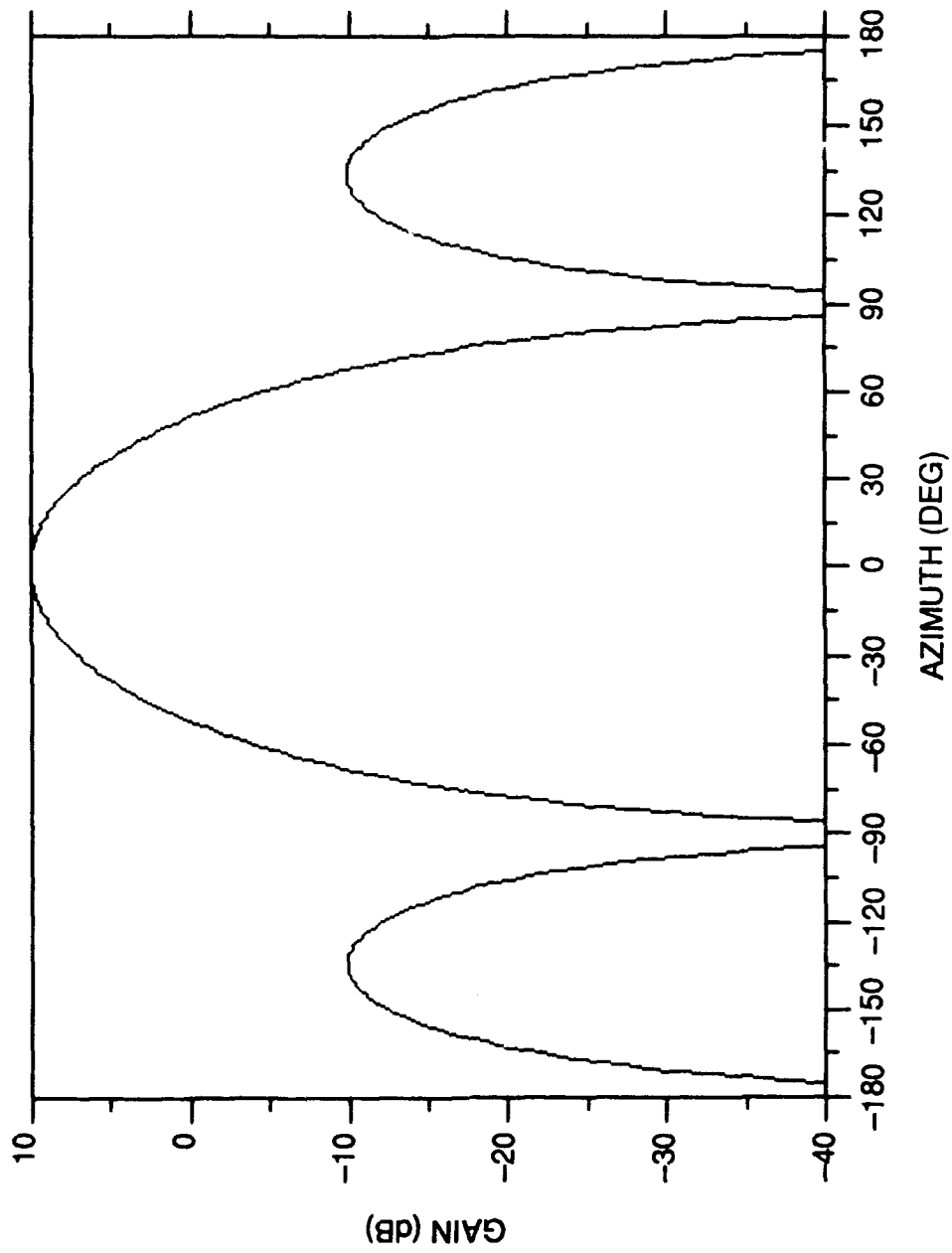


Figure 7. Theoretical Azimuthal Far-Field Pattern for a Subarray with Two Active Elements and Two Backpoles

THREE PATTERNS: SUBARRAY, ARRAY FACTOR, COMPLETE ARRAY D = 0.8 N = 36

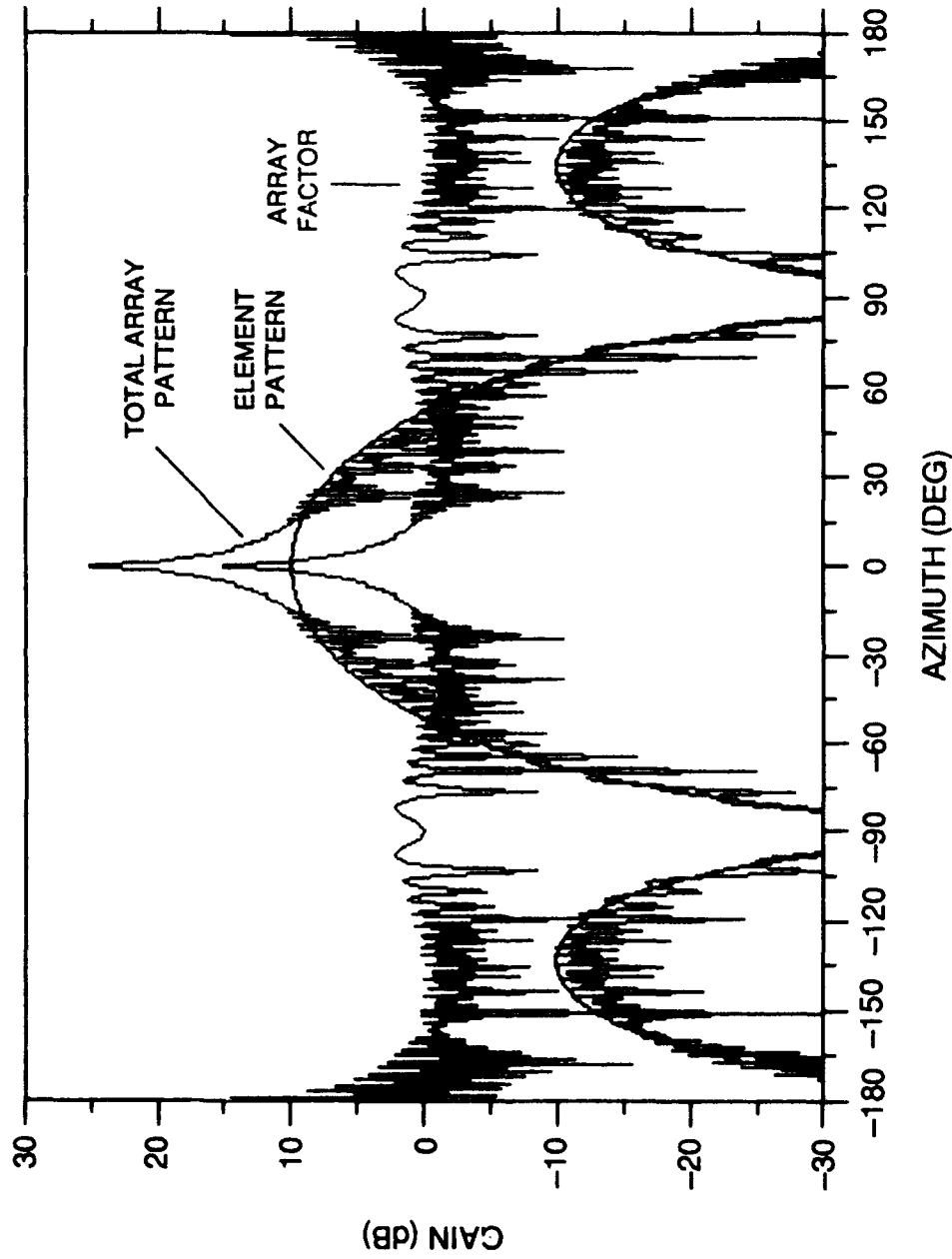


Figure 8. Array Factor, Subarray Pattern, and Resultant Radiation Pattern from Pattern Multiplication of Array Factor with the Subarray Pattern

THREE PATTERNS: SUBARRAY, ARRAY FACTOR, FULL ARRAY D = 0.8 N = 36 PHI0 = 20

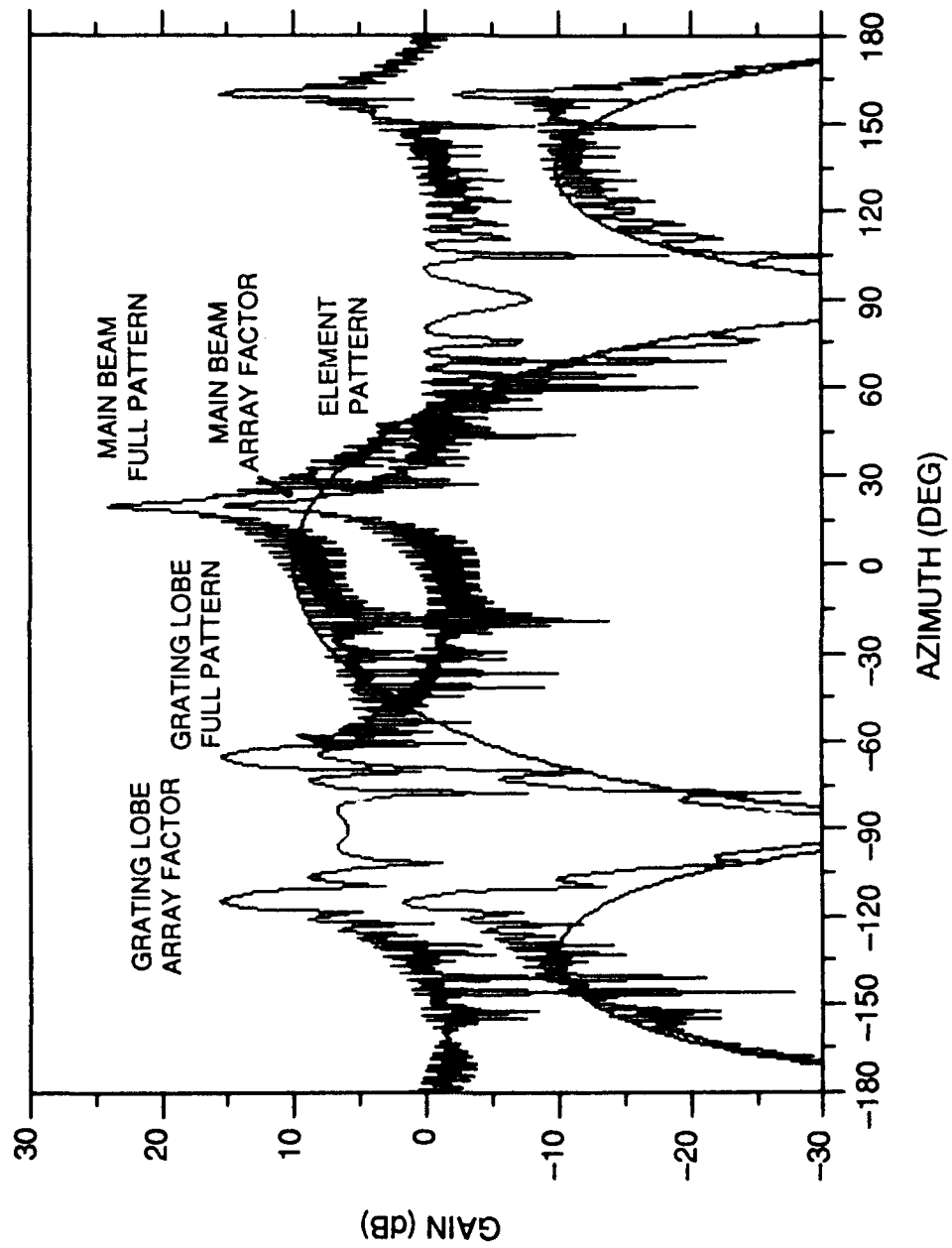


Figure 9. Array Factor, Subarray Pattern, and Resultant Radiation Pattern for Linear Array Scanned 20 Degrees Off Broadside

## 4. CALCULATIONS USING NUMERICAL ELECTROMAGNETICS CODE (NEC)

### 4.1 Introduction to NEC

The Numerical Electromagnetics Code (NEC)<sup>4</sup> is a computer program that uses the Method of Moments technique to predict the electromagnetic response of antennas and other metal structures. The physical structure to be analyzed is modeled using wire segments to approximate the correct shape and electrical characteristics. The required integral equations are then solved to determine the currents on an electromagnetically excited wire or structure. A step-by-step process using NEC was employed to model various monopole combinations. These structures were then combined to obtain the subarray and finally the complete arra

### 4.2 Far-Field Patterns Calculated with NEC

#### 4.2.1 VERTICAL MONOPOLE OVER PERFECT GROUND

A simple vertical monopole antenna was modeled first using NEC. The height of the antenna is 6 m and the element is driven by a 1 V source close to the ground. A calculation assuming a perfect ground plane was made to create a baseline and verify that the model is accurate. Next, an element over a finite ground plane was modeled using NEC. An option available with the NEC program to use Sommerfeld Integrals was employed. This method allows simulation of a structure very close to the ground. Various ground plane configurations and different frequencies were examined. Resultant patterns are shown in Figure 10 for both the perfectly conducting ground and a ground with finite conductivity representative of the earth at the Verona test site ( $\sigma = 0.1$  mhos/m,  $\epsilon = -30$ ).

#### 4.2.2 TWO ACTIVE ELEMENTS

A simulation of two active elements phased for a broadside configuration was computed and the field patterns calculated. This arrangement generates the common "figure-eight" pattern with nulls at  $\pm 90$  degrees in relation to broadside. The resultant azimuth pattern is shown in Figure 11.

#### 4.2.3 MONOPOLE WITH BACKPOLE

Similar to the process using theoretical methods, a backpole was paired with an active element to reduce the gain in the back half plane. The backpole in the NEC model is again located a quarter wavelength behind the active element. Ground wires are connected from the front element to the backpole. The backpole is not driven with a voltage but purely reacts in the passive manner described earlier in Section 3.3.2. This setup as in the earlier theoretical case results in an endfire configuration. The resultant pattern is shown in Figure 12. Note that nulls approximately 6 dB below the forward direction are formed at 180 degrees. In this and the following simulations the perfectly conducting ground plane model was used since only the azimuthal variation is under consideration.

---

4. Burke, G.J. and Poggio, A.J. (1980) *Numerical Electromagnetics Code (NEC)*, Tech. Doc. 116, Naval Oceans System Center.

VERTICAL MONOPOLES: 6 m HEIGHT, 12 MHz, 1. PERFECT GRND. 2. E = 0.1, D = 30.

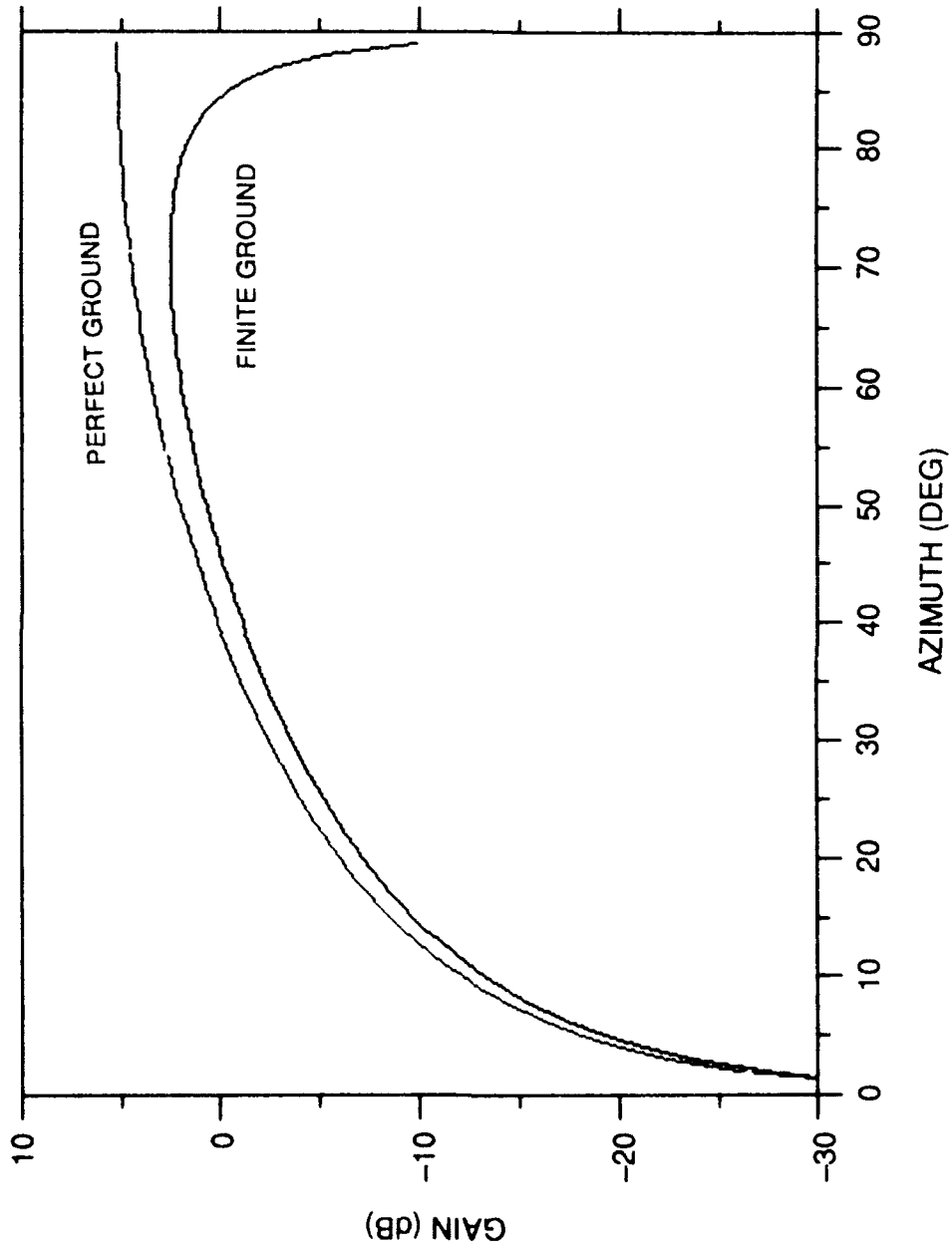


Figure 10. Elevation Radiation Pattern for a Simple Vertical monopole Over Perfect and Finite Ground Plaes Calculated with the NEC Modeling Program

PATTERN FOR TWO VERTICAL MONOPOLES PHASED BROADSIDE: NEC

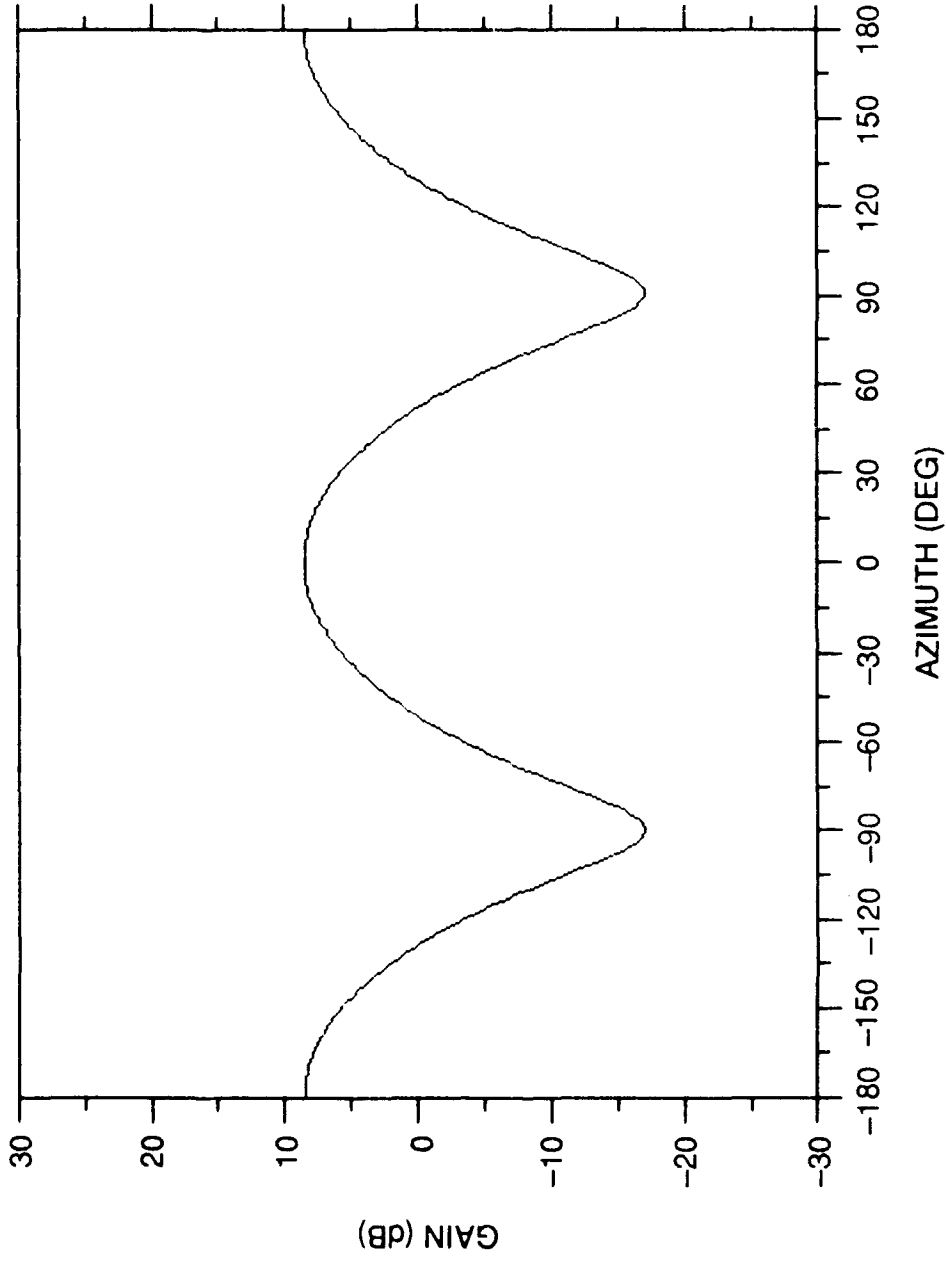


Figure 11. Azimuthal Pattern for a Two Element Subarray Phased Broadside Calculated with NEC

PATTERN FOR 1 ACTIVE ELEMENT AND 1 BACKPOLE: ENDFIRE CONFIGURATION

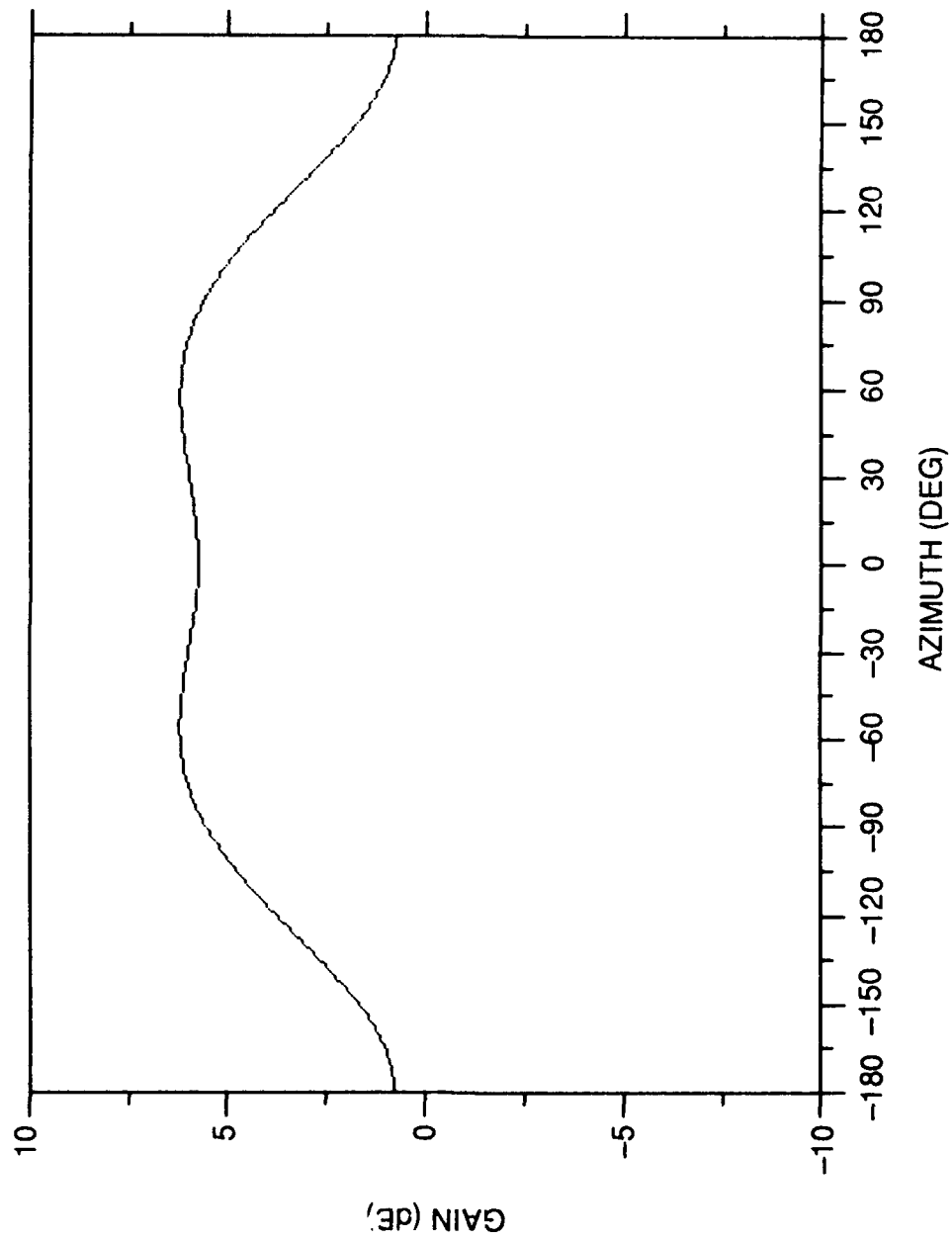


Figure 12. Azimuthal Radiation Pattern for a Two Element Subarray Phased Endfire Calculated Using the NEC Routine

#### 4.2.4 FULL SUBARRAY

The full subarray of two active elements and two backpoles was modeled next. Both active elements are driven in phase by 1 V sources. The resultant pattern for azimuthal scan is shown in Figure 13. This is the element pattern for the array. It is this pattern that can be multiplied by the array factor to create the full array pattern. The subarray pattern calculated using NEC shows nearly 15 dB of increased directivity in the forward direction (0 degrees) compared to behind the array (180 degrees).

#### 4.2.5 MODEL OF THE FULL ARRAY

The final modeling effort is naturally the full array of 36 subarrays and calculation of the composite element-array far-field patterns. Unfortunately, our version of the NEC code cannot accommodate structures as large as the full array of 36 elements. The largest array that could be handled in the program was 15 subarrays. The limitation of 15 subarrays decreases the gain, beamwidth, and number of lobes in the patterns. The overall response of the 15 element linear array model should still be a good representation of the 36 element array.

All active elements were fed with a 1 V source with no phase difference between elements causing the main beam of the pattern to occur in the broadside direction. The result is identical to a plane wave arriving that is oriented parallel to the array. The resultant azimuthal radiation pattern is shown in Figure 14. To determine the expected sidelobe behavior of the array, an amplitude weighting taper was used during calculation of the field pattern. This is done by factoring each of the voltage sources with a 32 dB cosine squared amplitude weight. The cosine squared function is only one of many possible weightings and was chosen because it does not broaden the main beam as much as other comparable weighting functions. The pattern for this simulation is shown in Figure 15. Notice that the sidelobe levels have been reduced from the uniform level of 13.2 dB shown in Figure 14 to 32 dB below the main beam. The main beam has broadened by 1 degree and about 3 dB of main beam amplitude loss has occurred. This loss and beam spread will cause a reduction in array resolution but it does not prevent adequate system performance.

### 5. FIELD MEASUREMENTS

#### 5.1 Introduction and Techniques

The HF test facility using the linear antenna array at Verona NY is currently in operation. Calibration and testing are complete and some preliminary clutter data have been collected. The pertinent pattern measurements made were the subarray pattern and the full 36 subarray, linear antenna pattern. The essential antenna information gained from these measurements includes the gain, average sidelobe level, beamwidth, grating lobe response, front to back ratio, and scan direction accuracy.

NEC - FULL SUBARRAY: TWO ELEMENTS AND TWO BACKPOLES PERF. GRND.

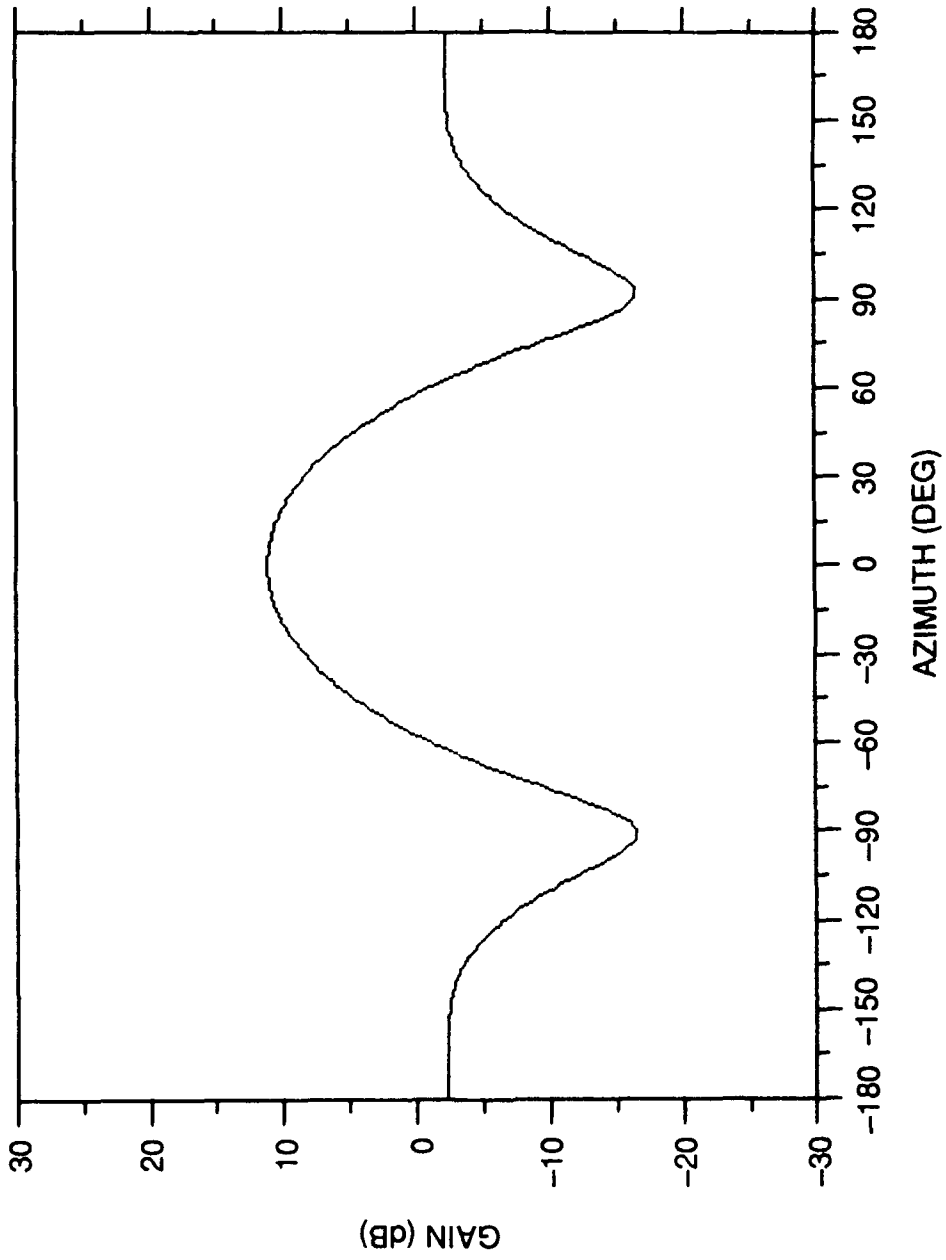


Figure 13. NEC Azimuthal Radiation Pattern for a Four Element Subarray Including Two Active Elements and Two Backpoles

NEC - LINEAR ARRAY: 15 SUBARRAYS, 12 MHz, NO TAPER 0 DEG

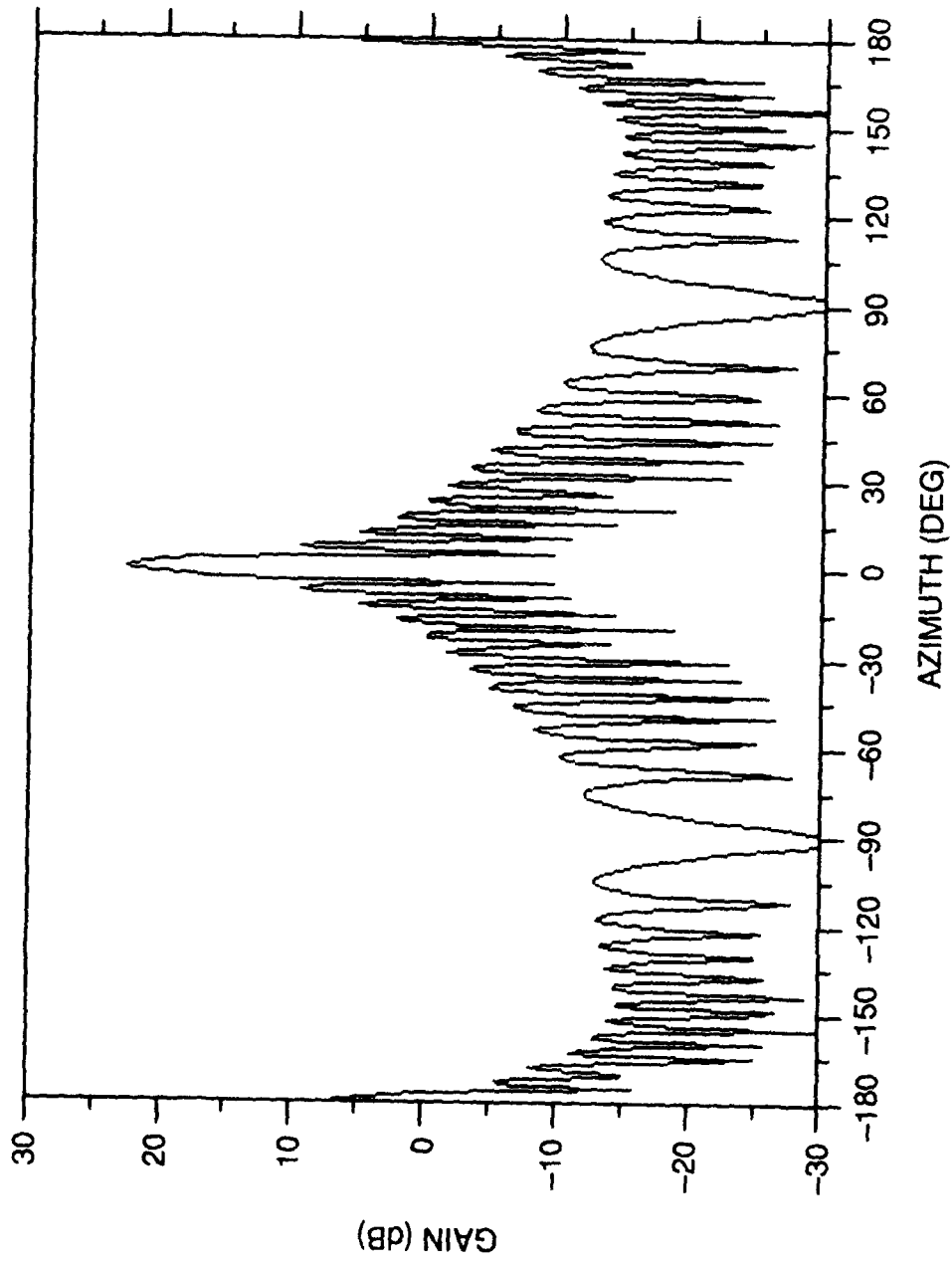


Figure 14. NEC Radiation Pattern for a Linear Array of 15 Subarrays, Including Two Active Elements and Two Backpoles. Zero degree scan angle

NEC - LINEAR ARRAY: 15 SUBARRAYS, 12 MHz, COS SQ. TAPER, 0 DEG

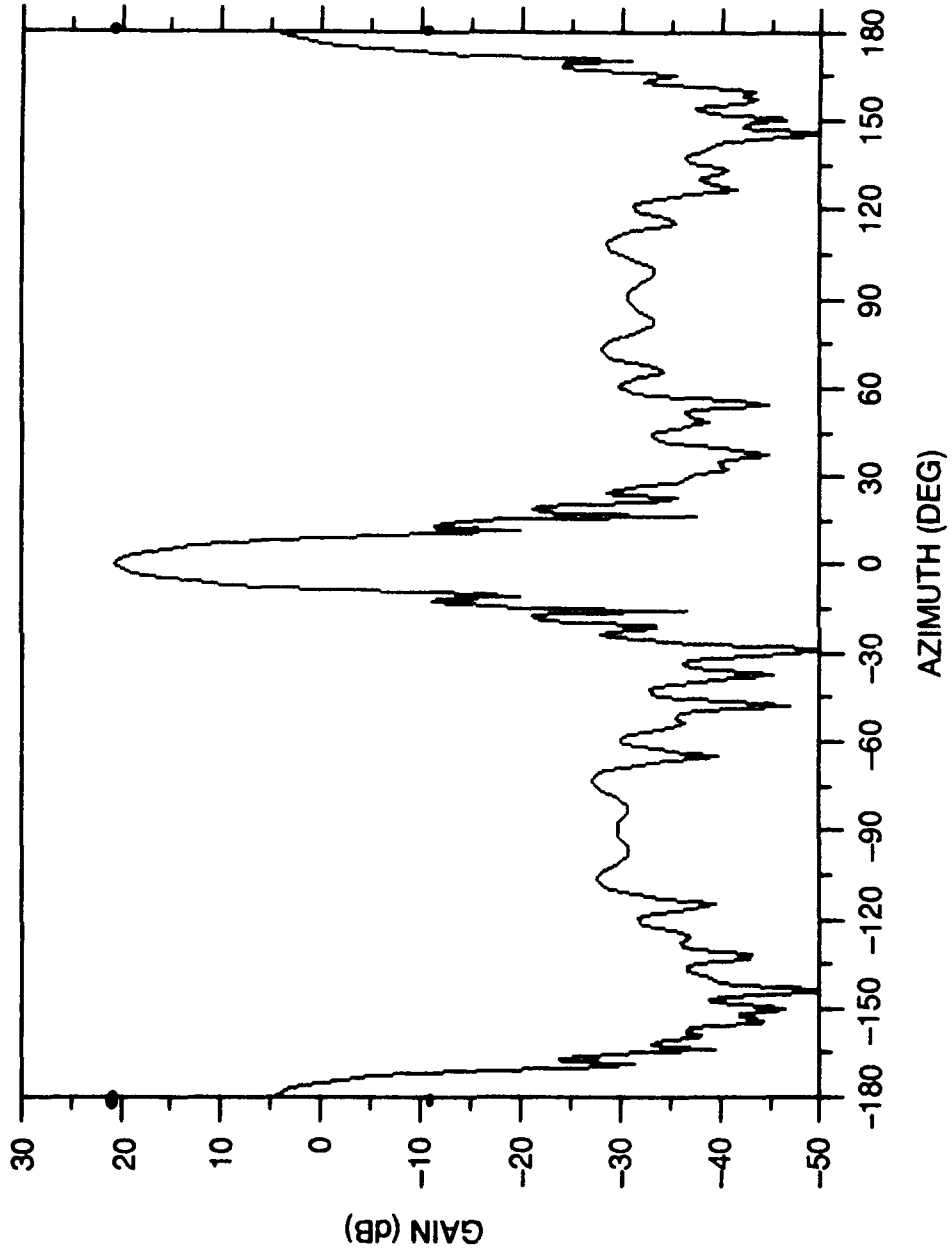


Figure 15. NEC Radiation Pattern for a Linear Array of 15 Subarrays, with a 32 dB Cosine Squared Weighting Taper

## 5.2 Measurement of the Subarray Pattern

The subarray pattern was determined by moving a continuous wave probe across the subarray aperture and plotting the received signal strength as a function of azimuth. Measurements were also made behind the array to determine the element directivity to the rear (180 degrees). Figure 16 shows the azimuthal element pattern for all the elements at a frequency of 10.205 MHz. Although not shown on this plot, the front to back ratio was also measured and is approximately 12 dB. Note that the subarray or element gain falls off rapidly for signals arriving at angles greater than 25 degrees from broadside. This falloff in gain permits the array to scan  $\pm 30$  degrees with the grating lobes reduced to at least 10 dB below the main beam.

## 5.3 Measurement of the Array Pattern

The field pattern for the full array was measured by scanning the array main beam past a CW signal transmitted from Ava, NY. Ava is located 21 miles away at a bearing from Verona of 31 degrees east of true north which corresponds to 21 degrees east of the array boresight. The power of the transmitted signal was 10 kW and the antenna used was a horizontal log periodic. The resultant full array pattern is shown in Figure 17. This pattern was obtained using measured data and applying a 32 dB cosine squared amplitude weighting function. Sidelobe response to the test signal is less than 32 dB RMS. Note that the beamwidth is greater than the 2.5 degrees available without the weighting taper but is still only approximately 4 degrees. This method of course does not account for the response of the subarray pattern but only the subarray pattern at a single bearing. Therefore, the actual gain will fall off as the scan angles become greater than 20 degrees as shown in Figure 16 by the subarray pattern.

## 6. ARRAY DESCRIPTION

The elements and pre-amplifiers for the linear antenna array were designed and built by RADC. The elements are constructed from electrical supply house materials, including 1-inch diameter rigid aluminum conduit, pvc pipe, pvc flanges, and pvc junction boxes. A diagram of the element is shown in Figure 18.

The signal output of each active monopole element is fed to a power combiner located halfway between the elements. The combined output is then band-pass filtered and sent to the pre-amplifier. Pre-amplifiers were deemed essential to overcome the sum of losses from cables, filters, and power combiners, which was calculated to be 15-20 dB. The gain of the pre-amplifiers was chosen to be 20 dB. The output of the pre-amplifier is carried through RG/215 coaxial cable to the receivers located in a central receive building. The building is located slightly off the middle of the array and 30 m behind the array. The RG/215-U used for the coaxial feed cable is low loss double shielded cable with an outside armor sheath. A unique aspect of this array is that each cable that connects a subarray back to one of the receivers, has a different length. The longest cable is approximately 1600 feet, while the shortest is 150 feet. Phase and amplitude differences for all channels are accounted for and adjusted *digitally during the beamforming process*. Figure 19 details the subarray configuration including the elements, power combiners, filters, and pre-amplifiers.

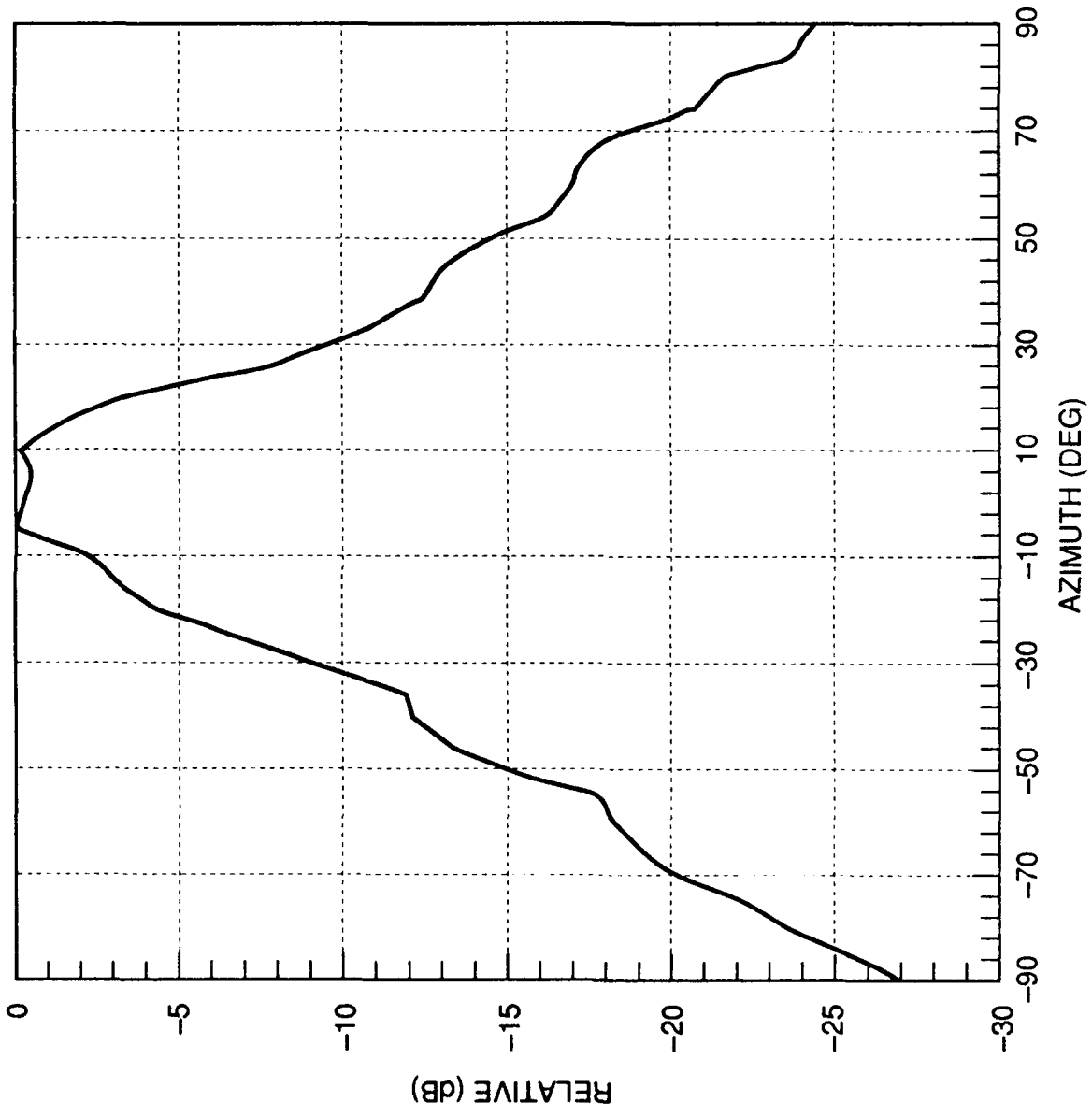


Figure 16. Measured Azimuthal Radiation Pattern for the Fielded Four Element Subarray

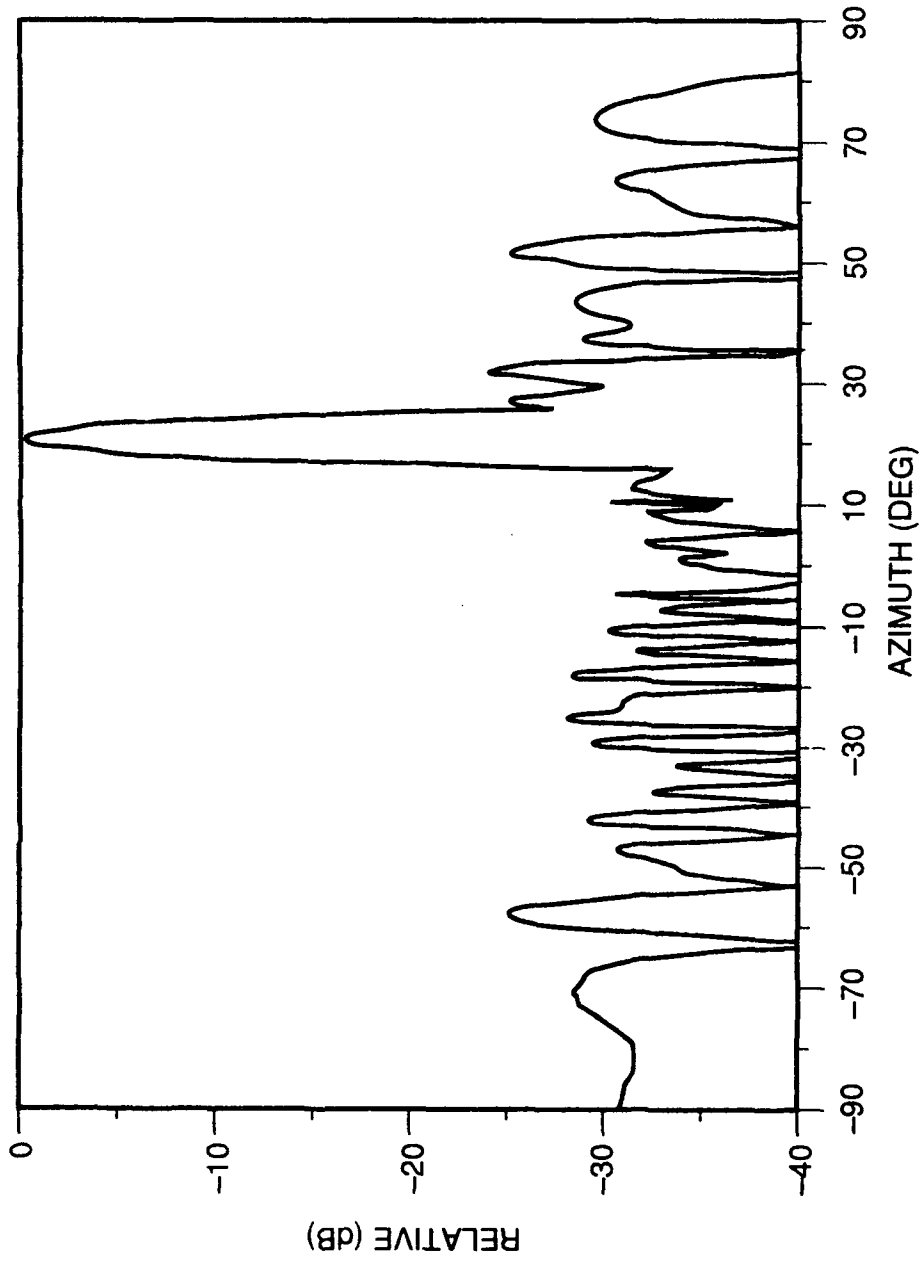


Figure 17. Measured 36 Element Linear Array Radiation Pattern Using the Ava Tx. Site as a source with a 32 dB cosine squared weighting.

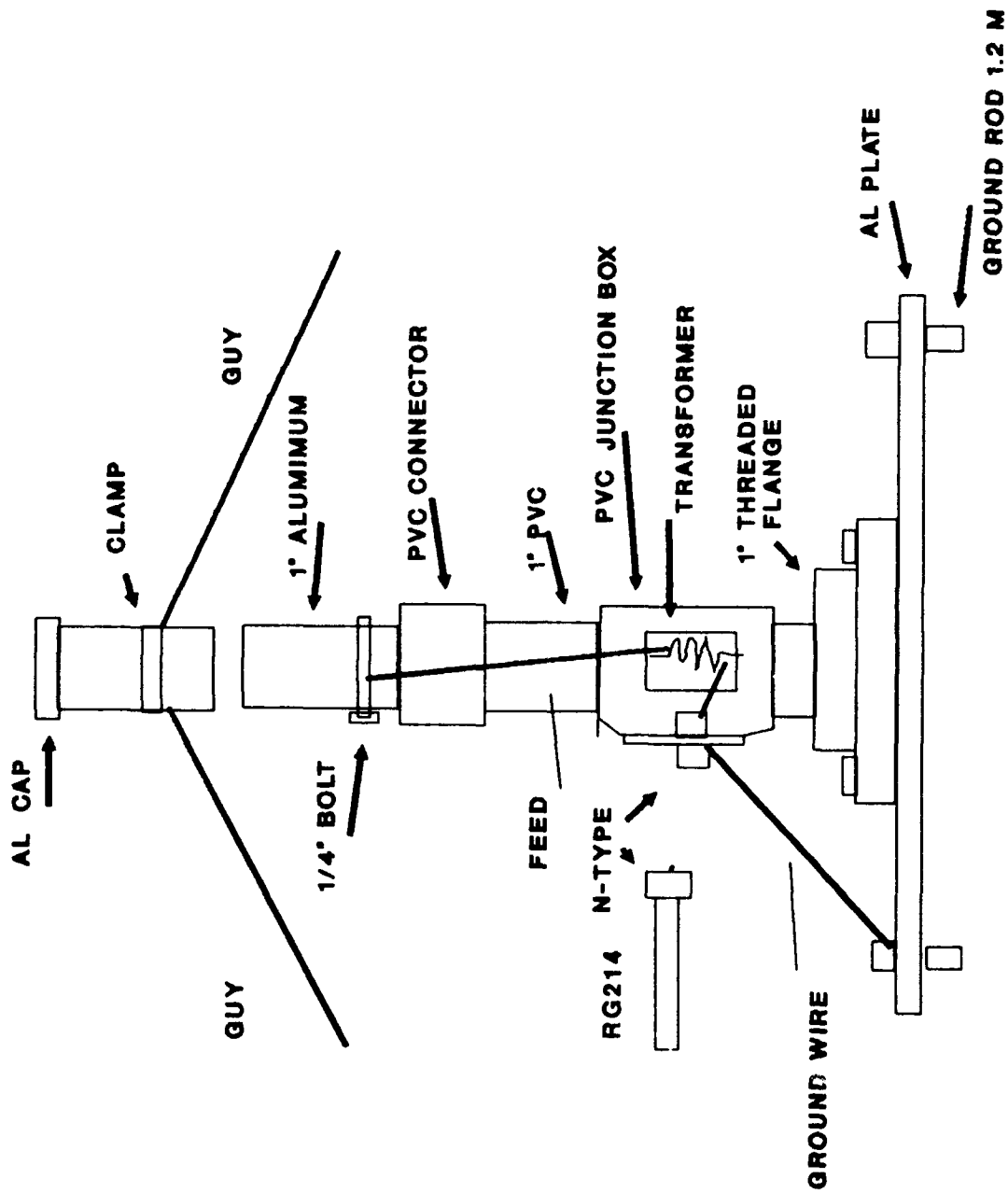
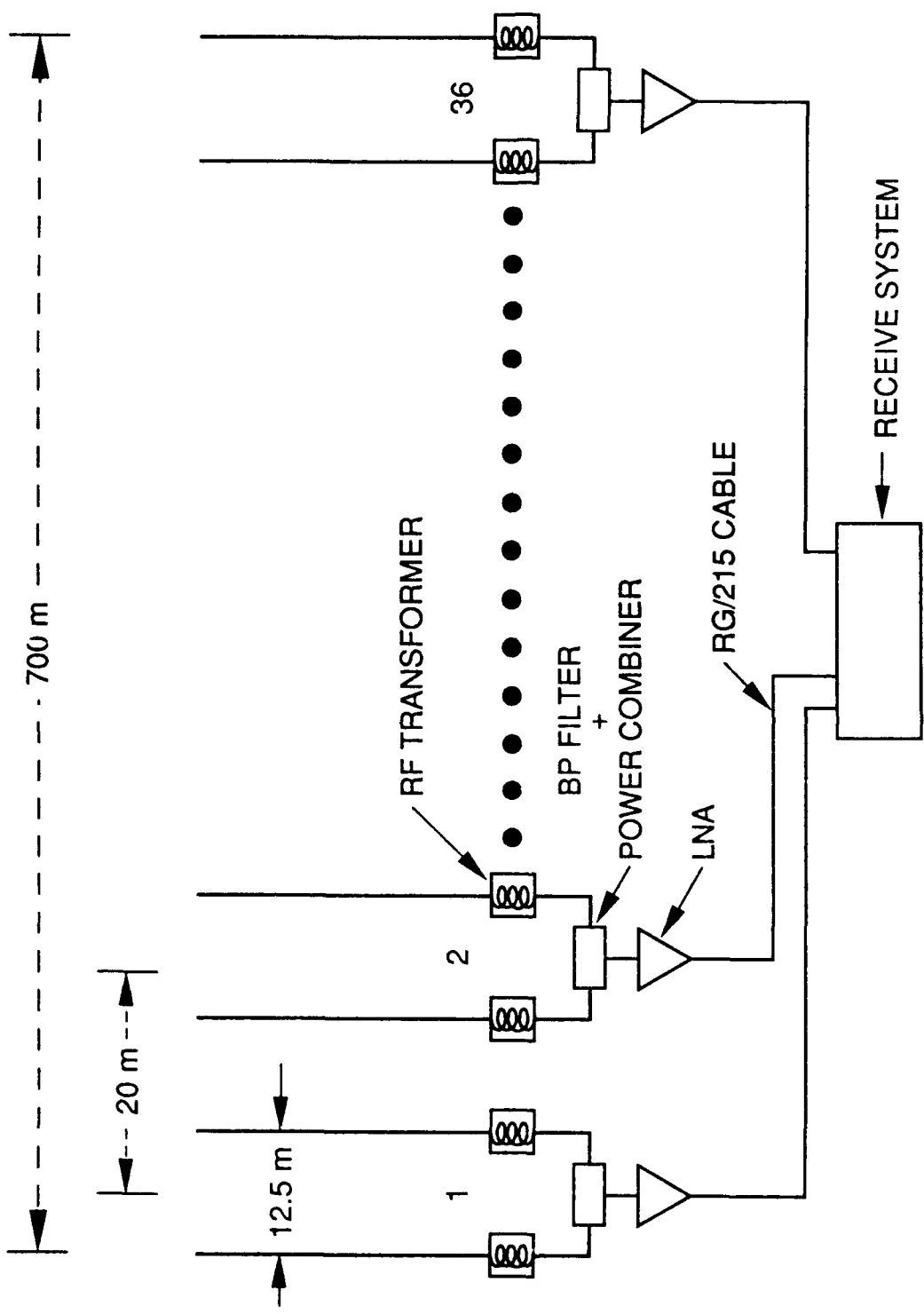


Figure 18. Schematic of One Active Element

VERONA LINEAR ARRAY  
SUBARRAY SCHEMATIC



\*PASSIVE BACKPOLE 6.25 m BEHIND EACH ELEMENT

Figure 19. Subarray Schematic

## 7. DISCUSSION

Once the required operating properties of the antenna, that is, gain, beamwidth, frequency band, etc. were specified, the antenna design effort and testing for this system, consisting of a three stage process, began. First, antenna theory was used to design an antenna that would meet these specifications. Second, numerical methods were used to test the theoretical designs and ensure that the designs met the performance specifications. Finally, pattern measurements of the fielded antenna were made to verify that the array performed as designed. Table 1 contains some of the major required specifications and the results obtained from each of the three techniques used. Although there are some minor differences, in general, the agreement between the numbers is quite good and shows that the use of theory and modeling techniques leads to the fabrication of an antenna with the properties needed for conducting meaningful experiments.

Table 1. Parameter Values from Each of Three Techniques

Parameter	Theoretical Calculations	NEC Calculations	Field Measurements
Gain (dB)	26	24	23
BW (dB)	2.5	3	≈ 2.5
Ave. SLL (dB)	32	≈ 30	32
F/B Ratio (dB)	> 20	15	12-14

## Refernces

1. Jordan, E., Edi. (1986) *Reference Data for Radio Engineers*, Howard W. Sams & Co.
2. Kraus, J.D. (1984) *Electromagnetics*, 3rd Ed., McGraw-Hill, p. 518.
3. Kraus, J.D. (1988) *Antennas*, McGraw-Hill.
4. Burke, G.J. and Poggio, A.J. (1980) *Numerical Electromagnetics Code (NEC)*, Tech. Doc. 116, Naval Oceans System Center.